Electron emission of Au nanoparticles embedded in ZnO for highly conductive oxide

Po-Shun Huang, Dong Hoe Kim, and Jung-Kun Lee

Citation: Applied Physics Letters **104**, 142102 (2014); doi: 10.1063/1.4870648

View online: http://dx.doi.org/10.1063/1.4870648

View Table of Contents: http://scitation.aip.org/content/aip/journal/apl/104/14?ver=pdfcov

Published by the AIP Publishing

Electron emission of Au nanoparticles embedded in ZnO for highly conductive oxide

Po-Shun Huang,[1] Dong Hoe Kim,[2] and Jung-Kun Lee[1,a)]
[1]Department of Mechanical Engineering and Materials Science, University of Pittsburgh, Pittsburgh, Pennsylvania 15261, USA
[2]Department of Materials Science and Engineering, Seoul National University, Seoul 151-744, South Korea

(Received 7 February 2014; accepted 25 March 2014; published online 7 April 2014)

We investigated the effect of embedded Au nanoparticles (Au NPs) on electrical properties of zinc oxide (ZnO) for highly conductive oxide semiconductor. Au NPs in ZnO films influenced both the structural and electrical properties of the mixture films. The electrical resistivity decreases by as much as five orders of magnitude. This is explained by the electron emission from Au NPs to the ZnO matrix. Temperature-dependent Hall effect measurements show that an electron emission mechanism changes from tunneling to thermionic emission at T = 180 K. The electron mobility in the mixture film is mainly limited by the grain boundaries at lower temperature (80-180 K), and the Au/ZnO heterogeneous interface at higher temperature (180-340 K). In addition to the electron emission, embedded Au NPs alter the ZnO matrix microstructure and improve the electron mobility. Compared to the undoped ZnO film, the carrier concentration of the Au NP-embedded ZnO film can be increased by as much as six orders of magnitude with a small change in the carrier mobility. This result suggests a way to circumvent the inherent tradeoff between the carrier concentration and the carrier mobility in transparent conductive oxide (TCO) materials.
 [http://dx.doi.org/10.1063/1.4870648]

ZnO is an abundant TCO material that possesses good electric and optical properties. These advantages promote ZnO as an attractive choice for many industrial applications including photovoltaics, luminescent displays, and thin film transistors. In order to reduce electric conductivity by increasing carrier concentration, IIIA dopants such as Al,[1–5] Ga,[6–8] and In,[9–12] have been incorporated into the ZnO lattice using several physical or chemical methods. In those studies of doped ZnO films, the carrier concentration reaches the range of 10^{19}–10^{20} cm^{-3}, the carrier mobility, however, is below 30 $cm^2/V\,s$. An inherent problem in these highly doped ZnO films is that: increasing the dopant level for high carrier concentration lead to an increase in the point defect density,[13] which could also serve as scattering centers for electrons. Since electron mobility of those doped ZnO films is mainly determined by point defects (ionized impurities) and extended defects (grain boundaries), highly doped ZnO with dense point defects exhibits low electron mobility.[14,15] This indicates a tradeoff between the carrier concentration and carrier mobility for those highly conductive ZnO films. To avoid this inherent problem, a sandwich-like structure of ZnO/metal/ZnO films have exhibited low resistivity when a metal mid-layer was inserted in the ZnO film.[16–18] Although previous studies suggest that this metal constituent within ZnO film can increase the carrier concentration of the ZnO matrix, the carrier mobility was confined within 10 $cm^2/V\,s$. It has been speculated that the nanostructured metal donates electrons to the ZnO matrix, but the surface of the metal constituent works as a new scattering center. However, a systematic analysis of a carrier transport mechanism in nanostructured metal-ZnO heterogeneous films have not been performed to date, and a way to mitigate the effect of the metal NP scattering on the carrier mobility of ZnO has not been reported.

In this study, temperature-dependent Hall effect measurements were employed to investigate electron injection and scattering in Au NP-embedded ZnO films. Au nanoparticles (NPs) were chosen because they have an excellent thermal stability that most metals do not possess.[19] The measurements provide an important clue as to the electron emission and transport mechanisms in Au NP embedded ZnO film. Our results demonstrate that Au NPs donate electrons into the ZnO matrix through the tunneling or thermionic emission. In this case, the highly crystalline ZnO matrix serves as a good transporting path that allows high electron mobility without the hindrance of scattering at point defects.

A stock solution for the sol-gel coating was composed of zinc acetate dihydrate dissolved in 2-methoxyethanol plus monoethanolamine (MEA) as a stabilizer. The solution was aged for 1 day at room temperature. ZnO thin films were spin-coated at a rate of 3000 rpm on surface-oxidized silicon substrates. The coating was repeated until the desired thickness is achieved. An e-beam evaporated Au mid-layer was then deposited on the ZnO bottom layer with the thickness controlled at 3, 5, 7, and 10 nm. Finally, the capping ZnO layer was spin-coated in the same way as mentioned. The samples were labeled as ZnO/ZnO (control sample without Au layer), ZnO/Au-3 nm, ZnO/Au-5 nm, ZnO/Au-7 nm, and ZnO/Au-10 nm. After coating, mixture films were placed in a tube furnace and thermally annealed at 500 °C in the N_2 atmosphere to convert the Au mid-layer into Au NPs embedded in ZnO films. The structural characterization was analyzed by X-ray diffraction (XRD, X'pert Diffractometer, Philips) at glancing angle with Cu-Kα radiation of $\lambda = 0.154$ nm. A cross-sectional view of Au NP embedded ZnO films was analyzed by transmission electron

a)Author to whom correspondence should be addressed. Electronic mail: jul37@pitt.edu

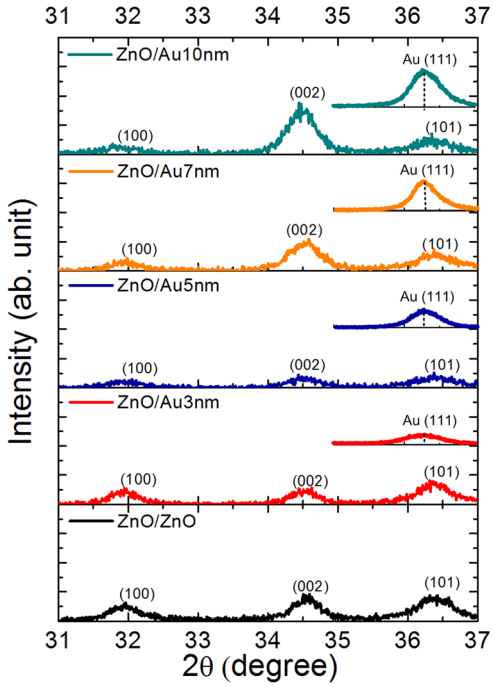

FIG. 1. XRD patterns of ZnO films with different thickness of the Au mid-layer (0, 3, 5, 7, and 10 nm). The insets show the intensity of the Au (111) diffraction peaks.

microscopy (TEM, JEM-2100F, JEOL). Temperature-dependent electrical properties of Au NP-embedded ZnO films were characterized via the Hall effect measurements with the Van der Pauw configuration (HMS-5000, Ecopia). During the measurements, a magnetic field of 0.5 T was applied to samples. The optical properties were analyzed by UV-Vis spectrometer (Lambda35, PerkinElmer).

Crystallographic structures of Au NP-embedded ZnO films are analyzed using XRD at glancing angle shown in Figure 1. ZnO/ZnO film exhibited typical hexagonal structure with a random orientation. However, as the initial Au mid-layer thickness increases the ZnO (002) peak intensity gradually rises to prominence with the Au (111) diffraction peak (see insets). This preferential growth is due to similar lattice parameters between ZnO (002) and Au (111).[20] It is noteworthy that the textured structure of semiconductor films is known to reduce the grain boundary scattering and enhance the carrier mobility consequently. An average Au NP crystallite sizes of ZnO/Au-3 nm, ZnO/Au-5 nm, ZnO/Au-7 nm, and ZnO/Au-10 nm films are calculated as 21.00, 21.04, 18.40, 18.42 nm according to the full-width at half maximum of Au (111) by Scherrer's formula. The similar crystallite size of all samples indicates that: an increase in the Au mid-layer thickness of the mixture films mainly changes the Au NP population density instead of the Au NP crystallite size.

The cross-sectional TEM image of the mixture films is shown in Figure 2. The total thickness of the mixture film is about 80 nm. Bright field images and backscattered electron images provide clear evidence of the Au NPs that are embedded in ZnO film. The size of the Au NPs in TEM images ranges from 15 nm to 30 nm, which agrees with the crystallite size calculated from XRD patterns. Elemental distribution mapping was performed by energy-dispersive spectroscopy (EDS). Au is found only near the center of the films, which suggests that those NPs are embedded in the ZnO matrix.

Electrical properties of Au NP embedded ZnO films as well as ZnO/ZnO and Au films are characterized by measuring the Hall effect. The temperature-dependent resistivity depicted in Figure 3(a) shows that Au NPs inside ZnO matrix brings a significant decreases in the electrical resistivity. For instance, when the initial Au mid-layer thickness reaches 10 nm, the resistivity of the film mixture is almost five orders of magnitude smaller than that of the ZnO/ZnO film at room temperature. The temperature dependence on resistivity for our mixture films is much stronger than that of the Au film. That gives a clue that the electric conduction mechanism involved in the mixture films is independent with that of the bulky metallic film, which is associated with the phonon scattering. Additionally, the mixture films demonstrate different temperature dependence as compared with the ZnO/ZnO film as well.

Furthermore, Figure 3(b) shows that a large decrease in the resistivity of mixture films is due to an increase in electron concentration. When Au NPs are embedded, the carrier concentration can be increased with the elevated temperature. The Arrhenius slopes (the carrier concentration vs. 1/T curves) of ZnO/Au-3 nm, ZnO/Au-5 nm, ZnO/Au-7 nm, and ZnO/Au-10 nm films are similar, regardless of the Au mid-layer thickness. Arrhenius plots indicate that free electrons of our mixture films have physical origin different either from Au or ZnO/ZnO films. A few recent studies on metal NP-embedded TCO films suggested that electrons can be emitted from metal NPs to the oxide matrix,[17] but the activation energy of the emission process was not experimentally presented. A work function of Au (~5.1 eV) is slightly larger than that of undoped ZnO (4.6 eV–4.9 eV) and the Schottky barrier is formed at the Au-ZnO interface in Au NP-embedded ZnO films. Hence,

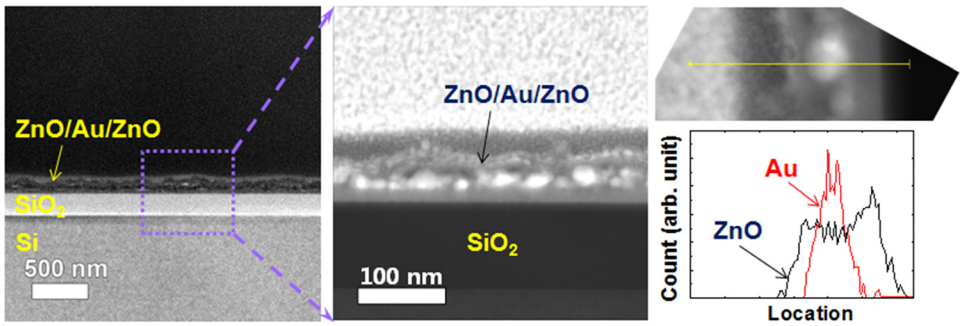

FIG. 2. TEM images of the ZnO/Au-5 nm; (a) bright field image of ZnO/Au/ZnO film deposited on SiO_2/Si substrate, (b) high-angle annular dark-field (HAADF) image of the same film at higher magnification, and (c) the elemental distribution of the same film along the yellow line measured from the EDS analysis.

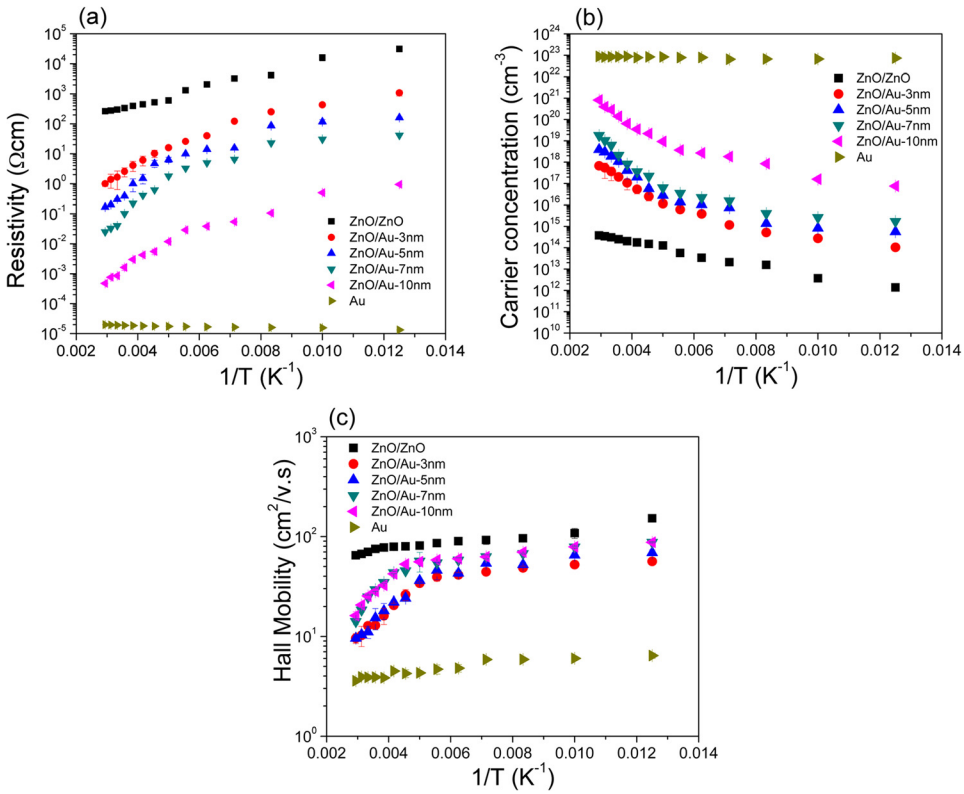

FIG. 3. The temperature-dependent electrical properties of Au NP embedded ZnO films with varied initial Au thicknesses deposited by e-beam evaporator, plus ZnO/ZnO film (~80 nm thick) and pure Au film (~10 nm thick); (a) electrical resistivity, (b) carrier concentration, and (c) carrier mobility.

electron emission from the Au NP to the ZnO matrix needs to overcome the Schottky barrier at the Au-ZnO interface. The Arrhenius slope in Figure 3(b) shows that the activation energy for free electron generation is about 188 meV for all Au NP-embedded ZnO films at $T > 180$ K. The activation energy of 188 meV is the height of Schottky barrier at Au-ZnO interface, which quantitatively corresponds to a difference in the work functions between Au and ZnO. This reveals that the high electron concentration of the Au NP-embedded ZnO film is attributed to the thermionic emission of electrons from Au NPs to ZnO matrix. However, when the temperature is lower than 180 K, energetic barrier heights decrease to 40–50 meV. This energetic barrier change indicates that the thermionic emission at the Au-ZnO interface is no longer the primary carrier emission mechanism in the low temperature regime. Due to the low thermal energy of free electrons in Au NPs at low temperature, the thermionic emission probability becomes negligible. Instead, electrons in Au NPs cross through the interface barrier via tunneling, which reduces the activation energy for the electron emission.[21] It is noted that all samples show similar activation energies originating from the same mechanism, regardless of the initial Au mid-layer thickness. Given that the initial Au mid-layer only influences the Au NP population density, the similar activation energies of all samples suggest that more electrons can go across the Au-ZnO interface in the mixture film with the thicker initial Au mid-layer.

The electron transport is limited by several possible scattering mechanisms such as grain boundaries, ionized impurities, phonons and extended defects (dislocations or stacking faults), and neutral centers.[22] In an undoped ZnO film, the grain boundary scattering is dominant over other scattering mechanisms.[23,24] The temperature-dependent electron mobility of the Au NP-embedded ZnO film is shown in Figure 3(c). In a low temperature region (80–180 K), the slopes in mobility vs. 1/T curves of Au NP-embedded and ZnO/ZnO films are very similar, which means that the electron mobility is determined by the grain boundary scattering. The mobility of ZnO/Au-10 nm film is larger than that of ZnO/Au-3 nm film due to the better textured structure (see Figure 1).

However, as the temperature exceeds 180 K, the slope in mobility vs. 1/T curves of mixture films is several times larger than that of the pure ZnO. Hence, the electron mobility of mixture films is significantly lower than that of the ZnO/ZnO film. To examine the effect of Au-ZnO interface on the carrier scattering at $T > 180$ K, we changed the thicknesses of ZnO films.

Figure 4 shows the temperature dependence of the carrier concentration and carrier mobility in Au NP-embedded

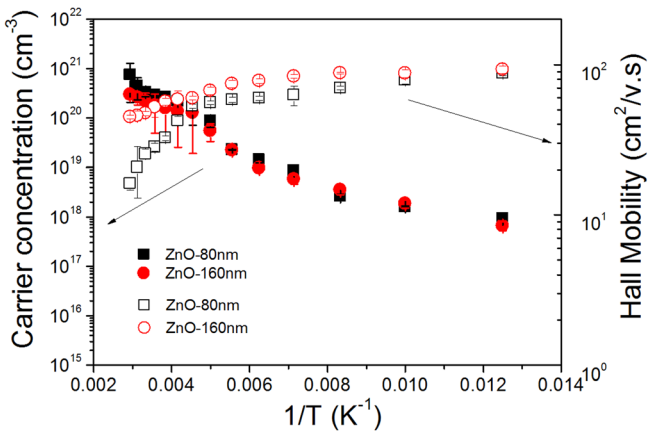

FIG. 4. Temperature-dependent carrier concentration and carrier mobility of Au NP added ZnO films with varied ZnO layer thicknesses. The solid square and circle refer to the carrier concentration, and the hollow square and circle present the carrier mobility (the initial Au layer thickness is 10 nm for every sample).

ZnO films with total thicknesses of 80 nm and 160 nm. In both films, the initial Au mid-layer thickness is fixed at 10 nm. Both films exhibit very similar carrier mobility at $T < 180$ K. When the temperature exceeds 180 K, the electron mobility of the 160 nm thick film is much larger than that of the 80 nm thick film. A large mobility difference between these two mixture films at room temperature demonstrates that the electron scattering centers in Au NP embedded ZnO at $T > 180$ K are not grain boundaries or other intrinsic defects in the ZnO matrix. Given that the increase in the ZnO layer thickness reduces the Au-ZnO interface area per unit volume, electrons scattering in the mixture film at room temperature is attributed to the presence of the Au-ZnO interface. The electron mobility of 160 nm thick ZnO/Au-10 nm film with a carrier concentration of $2.2 \times 10^{20}\,cm^{-3}$ is increased to $47\,cm^2/V\,s$. Compared with the ZnO/ZnO film ($n = 3.0 \times 10^{14}\,cm^{-3}$, $\mu = 70\,cm^2/V\,s$), the carrier concentration of Au NP embedded ZnO film becomes six orders of the magnitude larger, but the mobility of Au NP embedded ZnO film decreases by only 23%. The results in this study shows that the carrier concentration and mobility of the mixture films can be independently controlled without the hindrance of the ionized impurity scattering that inherently exists in highly doped ZnO films.

We also measured the optical properties of the films. The transmittance spectra (not shown) of mixture films range from 68% to 85% at the wavelength of 500 nm, depending on the amount of Au NPs. As the initial Au layer thickness increases, the transmittance of the film decreases. In comparison, the ZnO/ZnO film exhibits the transmittance of 93% for light with the same wavelength (500 nm).

In summary, electrical properties of Au NP embedded ZnO films are examined systematically. An increase in the thickness of the initial Au mid-layer in the mixture film increases the density of Au NPs instead of their size. The free electron concentration of Au NP embedded ZnO films is dramatically increased due to the electron emission from Au NPs to the ZnO matrix. At $T > 180$ K, Au NP electrons are thermally emitted across the Schottky barrier at the An-ZnO interface, where the energetic height is approximately 188 meV. In the lower temperature region ($T = 80$–180 K), Au NPs donate electrons to the ZnO matrix through tunneling phenomena. A relatively small change in the carrier mobility between ZnO/ZnO film and ZnO/Au-10 nm film shows that the ZnO matrix provides a good electron transport path for electrons that are emitted from Au NPs. This result offers a design rule for highly conductive TCO that is free from the traditional tradeoff between the carrier concentration and the carrier mobility.

This work has been funded by National Science Foundation (Grant No. DMR-0847319 and CBET-1235979). J.K. Lee also acknowledges World Class University program through National Research Foundation of Korea.

[1]X. Jiang, F. L. Wong, M. K. Fung, and S. T. Lee, Appl. Phys. Lett. **83**, 1875 (2003).
[2]V. Musat, B. Teixeira, E. Fortunato, R. C. C. Monteiro, and P. Vilarinho, Surf. Coat. Techonol. **180–181**, 659 (2004).
[3]J.-P. Lin and J.-M. Wu, Appl. Phys. Lett. **92**, 134103 (2008).
[4]W. M. Tsang, F. L. Wong, M. K. Fung, J. C. Chang, C. S. Lee, and S. T. Lee, Thin Solid Films **517**, 891 (2008).
[5]K.-M. Lin, H.-C. Chen, Y.-Y. Chen, and K.-Y Chou, J. Sol-Gel Sci. Technol. **55**, 369 (2010).
[6]H. Gómez and M. de la L. Olvera, Mater. Sci. Eng., B **134**, 20 (2006).
[7]S. Jeong, Y.-G. Ha, J. Moon, A. Fachetti, and T. J. Marks, Adv. Mater. **22**, 1346 (2010).
[8]S.-Y. Huang, T.-C. Chang, M.-C. Chen, S.-W. Tsao, S.-C. Chen, C.-T. Tsai, and H.-P. Lo, Solid-State Electron. **61**, 96 (2011).
[9]C. Gi Choi, S.-J. Seo, and B.-S. Bae, Electrochem. Solid-State Lett. **11**(1), H7 (2008).
[10]K. J. Chen, F. Y. Hung, S. J. Chang, and Z. S. Hu, Appl. Surf. Sci. **255**, 6308 (2009).
[11]E. J. Luna-Arredondo, A. Maldonado, R. Asomoza, D. R. Acosta, M. A. Meléndez-Lira, and M. de la L. Olvera, Thin Solid Films **490**, 132 (2005).
[12]A. Maldonado, M. de la Luz Olvera, S. Tirado Guerra, and R. Asomoza, Sol. Energy Mater. Sol. Cells **82**, 75 (2004).
[13]J. H. Noh, H. S. Jung, J.-K. Lee, J. Y. Kim, C. M. Cho, J.-S. An, and K. S. Hong, J. Appl. Phys. **104**, 073706 (2008).
[14]K. Ellmer, J. Phys. D: Appl. Phys. **34**, 3097 (2001).
[15]K. Ellmer, A. Klein, and B. Rech, "Transparent Conductive Zinc Oxide: Basics and Applications," in *Thin Film Solar Cells* (Springer, 2008).
[16]H. Han, N. D. Theodore, and T. L. Alford, J. Appl. Phys. **103**, 013708 (2008).
[17]K. Sivaramakrishnan and T. L. Alford, Appl. Phys. Lett. **96**, 201109 (2010).
[18]K. Sivaramakrishnan, N. D. Theodore, J. F. Moulder, and T. L. Alford, J. Appl. Phys. **106**, 063510 (2009).
[19]C. Corti and R. Holliday, *Gold Science and Applications*, 1st ed. (CRC Press, 2010), p. 167.
[20]L. V. Basbanes, *Advanced Materials Research Trends* (Nova Science Publishers, Inc., 2007).
[21]P. Sheng, E. K. Sichel, and J. I. Gittleman, Phys. Rev. Lett. **40**, 1197 (1978).
[22]H. Liu, V. Avrutin, N. Izyumskaya, U. Ozgur, and H. Morkoc, Superlattices Microstruct. **48**, 458 (2010).
[23]S. Calnan and A. N. Tiwari, Thin Solid Films **518**, 1839 (2010).
[24]K. Ellmer and R. Mientus, Thin Solid Films **516**, 4620 (2008).